

Groove Gap Waveguide (GGW) H-plane Horn Antenna and a Method for Its Back lobe Suppression

F. Ahmadvard, S. A. Razavi Parizi

Department of Electrical and Computer Engineering, Graduate University of Advanced Technology
Kerman, Iran, fahmadfard@yahoo.com, s.razaviparizi@kgut.ac.ir
Corresponding author: s.razaviparizi@kgut.ac.ir

Abstract- recently a new structure called groove gap waveguide (GGW) is introduced to implement low loss microwave component devices especially for millimeter wave applications. This paper presents a new type of H-plane horn antenna making use of this new technology in which backward radiation is significantly suppressed by introducing a high impedance surface at the antenna aperture. The high impedance surface that we used as the back lobe suppressor is a corrugated surface. The designed antenna is simulated by HFSS and its radiation performance is compared with an ordinary GGW H-plane horn in which no back lobe suppression mechanism is used. Results show a significant improvement in back lobe suppression and gain enhancement by the proposed structure.

Index Terms- Groove Gap Waveguide (GGW) Horn Antenna, Back lobe Suppression.

I. INTRODUCTION

In recent years, a new structure called groove gap-waveguide (GGW) is presented for implementation of microwave component devices especially at millimeter wave frequencies [1-4]. A GGW due to lower losses than microstrip like structures as well as easier fabrication process than metallic waveguides (at high frequencies) has recently attracted the attention of researchers for the design and manufacture of microwave devices and antennas.

In GGW there are two PEC and PMC parallel plates including a contrived PEC path (a groove) in the plate of PMC. The PMC surface is realized by a textured surface which is usually implemented by periodic metal pins known as "Fakir Bed of nails" [5-6]. In this case the wave propagation is possible along this PEC path (i. e. inside the groove) without any need to electrical contact between upper and lower plates which makes it interesting in manufacturing point of view especially at high frequencies. Moreover, GGW structure is completely closed and does not suffer from parasitic radiation. This structure due to release of the wave power in free space, has lower l

osses and also capable of carrying more power than microstrip and SIW structures. Thus, it can be a good candidate for realization of antennas especially at high frequencies.

A GGW is expected to allow the propagation of modes in a similar way as in hollow rectangular waveguide with cut off frequency given by the groove dimensions. Due to these similarities, GGW can also be used in the design of microwave components and antennas that are implemented by hollow rectangular waveguides. The superiority of GGW relative to hollow rectangular waveguide can be sensed in fabrication process at high frequency applications. Since in GGW there is no need to electrical contact between plates, the fabrication process is straight forward however in the hollow rectangular waveguide the fabrication process is so challenging at high frequencies due to the need of fine electrical contact between metal plates. Up to now, there are only few works on implementation of microwave components and antennas based on this new technology. Some examples of this can be found in [7-10].

In this paper an H-plane horn antenna is designed based on groove gap waveguide technology. In the proposed antenna, the backward radiation is suppressed using a high impedance surface (corrugated surface) at the antenna aperture which has resulted in antenna gain enhancement. The radiation properties of proposed antenna are compared with those of an ordinary GGW H-plane horn in which no back lobe suppressor is used. Results show a significant improvement in back lobe suppression and gain enhancement by the proposed structure.

II. ANTENNA STRUCTURE AND ITS OPERATION PRINCIPLE

Fig.1 shows the structure of a GGW H-plane horn antenna and its geometrical parameters. In Fig. 1 (a) the ordinary GGW horn is shown in which no back lobe suppressor is used. In Fig. 1(b) corrugations are introduced at the antenna aperture working, as shown later, as a back lobe suppression mechanism. We see that the proposed antenna is realized by an open end horn shaped groove located inside a bed of nails. A metal plate is also placed on the entire structure. There is an air gap between upper plate and pin surface (see the structure side view in Fig. 1(c)). In this topology the fields are coupled to the groove by a probe and then propagate along it until they reach its open end, i.e. the antenna aperture, through which they radiate to the outer space. Since the upper face of bed of nails acts as a PMC the propagating fields are well confined to the groove area without any need to electrical contact between upper plate and lower layer. This fact makes the antenna fabrication straight forward especially at high frequencies.

In Fig. 2 the field distribution inside the antenna structure is illustrated and the above discretion can be clearly observed. It should be noted that the PMC surface is frequency dependent, i. e. there is a limited frequency band over which the fields propagation along it is stopped. This frequency band is called stop band which limits the antenna operating bandwidth.

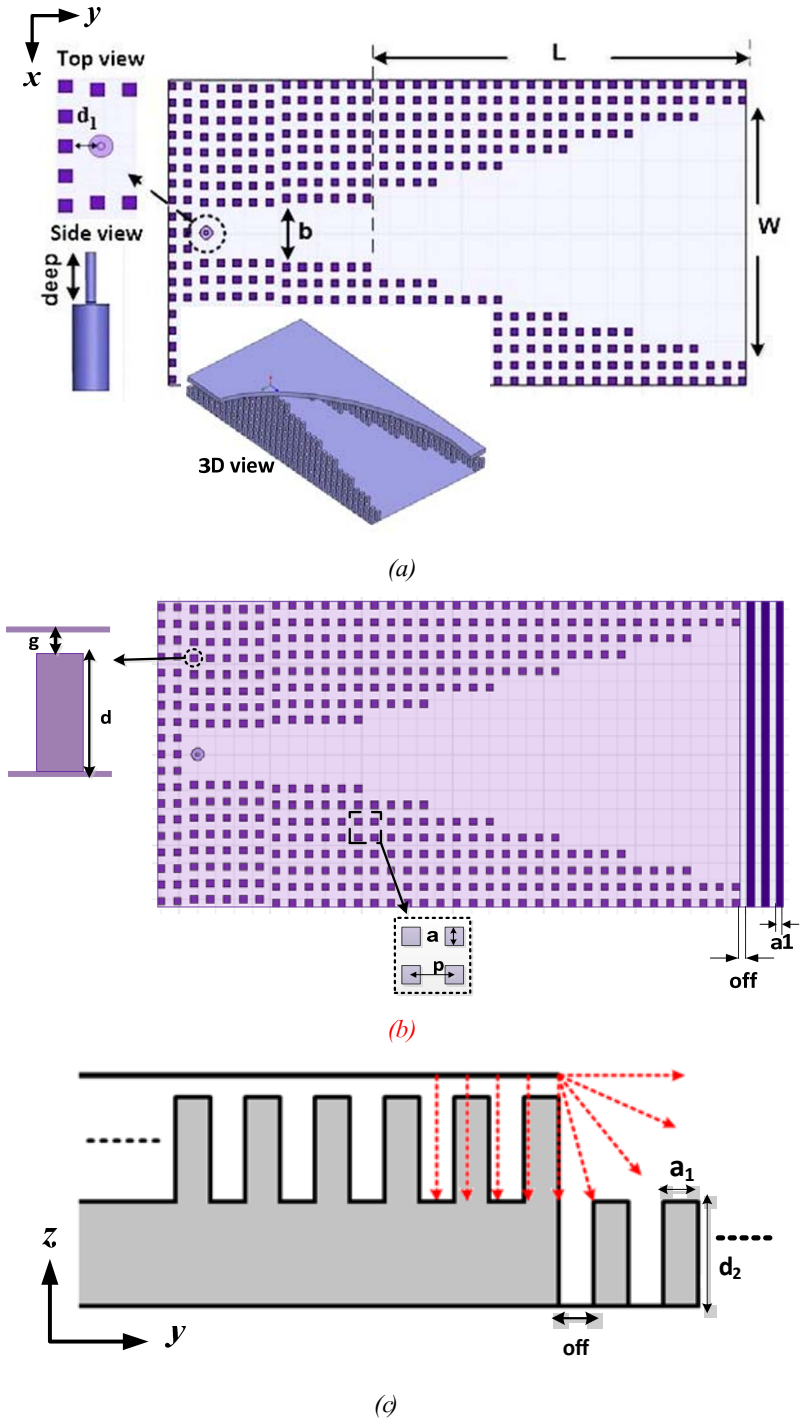


Fig. 1. The structure of proposed GGW H-plane horn antenna. (a) without any back lobe suppression Mechanism, (b) Using corrugations as a back lobe suppression mechanism (top view) and (c) Side view of Fig. 1(b).

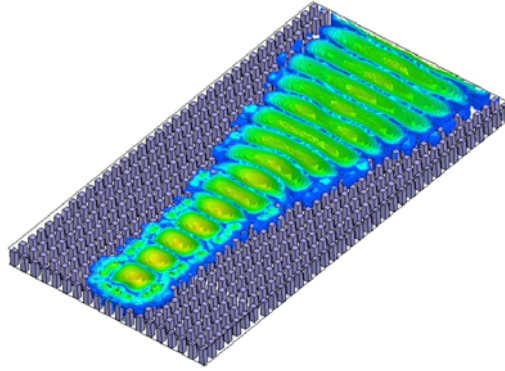


Fig. 2. The field distribution inside the proposed GGW H-plane horn antenna.

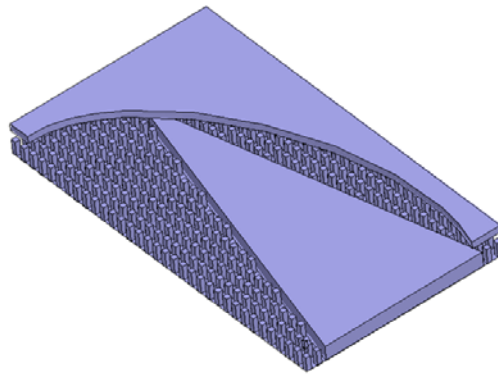


Fig. 3. The 3D view of RGW H-plane horn antenna presented in [10].

The dimensions pin surface and air gap are selected base on the rules presented in [11] in order to create a stop band over which the antenna is supposed to operate. The dimensions of the horn flared part are also chosen using the rules in [12] in order to have maximum directivity. The width of GGW rectangular feeding waveguide should be also chosen so that its dominant mode (TE_{10} mode) cut of frequency is lower than the desired frequency range. As depicted in Fig. 1, the GGW rectangular waveguide is fed by a probe. In order to have proper impedance matching, the probe length and its distance with the closed end of the waveguide should be chosen about a quarter wavelength. However these values are considered as initial values and fine tuning is needed to obtain the best performance.

Base on the rules presented in [11], the pins height, d , is approximately $\bar{\epsilon}/4$ where $\bar{\epsilon}$ is the center frequency of pin surface stop band. So the antenna aperture thickness which mainly determined by $\bar{\epsilon}d$ is about $\bar{\epsilon}/4$ satisfying the rule that says: for an H-plane horn antenna in order to get proper radiation performance the aperture thickness should be more than $\bar{\epsilon}/6$ [13-14]. In ridge gap waveguide (RGW) H-plane horn presented in [10] (which is shown in Fig. 3), the aperture thickness is determined by the air gap, $\bar{\epsilon}g$. In this case, in order to satisfy the above rule, the air gap thickness should be increased which results in narrow top band and consequently narrow bandwidth for the antenna. By the RGW H-

Table I. GEOMETRICAL PARAMETERS OF THE DESIGNED ANTENNAS

Parameter	Value (mm) In Fig.1(a)	Value (mm) In Fig.1(b)
L	159.5	159.5
W	71	71
b	15	15
a	2	2
b	15	15
g	1	1
p	4.5	4.5
d	6	6
d_2	-	6
deep	3.5	3
d_1	3.25	4.5
a_1	-	2
off	-	2

plane horn antenna presented in [10] only 1-2% bandwidth can be achieved. But here by using GGW technology, as mentioned before, the antenna aperture thickness can be kept larger than $\lambda/6$ for any value of g (even $g=0$) which gives us this possibility to make the stop band wide enough so that it does not affect the antenna bandwidth.

In the proposed structure shown in Fig. 1(a) the antenna radiates toward \hat{y} direction and the diffraction from upper and lower edges of aperture contributes to the antenna backward radiation. In order to suppress the backward radiation and consequently improve the antenna gain, as shown in Figs. 1 (b, c), we used two rows of corrugations (a high impedance surface) at the antenna aperture. In this case, as schematically depicted in Fig. 1 (c), the three rows of pins create a high impedance condition in front of the antenna aperture preventing the outgoing wave to propagate along forward direction (i.e. \hat{y} axis) leading to upward radiation of antenna (i.e. toward \hat{z} axis). In this case the antenna aperture edges are chocked between a large ground plane (i.e. antenna top plate) and a high impedance surface (realize by the three rows of pins). As a result, the diffraction phenomenon from the aperture edges and consequently the backward radiation drops leading to gain enhancement compared to the ordinary form shown in Fig. 1(a). So we see that the high impedance surface introduced at the antenna aperture, as shown in Figs. 1 (b, c), acts as a back lobe suppressor. The dimensions of corrugations are chosen based on the rules presented in [15] in order to act as a high impedance surface at the antenna operating frequency. The depth of corrugations should be about $\lambda/4$ where λ is the antenna center operating frequency. The parameters d_2 and off_1 should be adjusted to obtain proper impedance matching.

A sample of each proposed structure presented in Fig. 1 is designed and simulated using both HFSS and CST (for comparison) to operate at Ku band. The dimensions of designed antennas are listed in TABLE I. The simulation results are discussed in the next section.

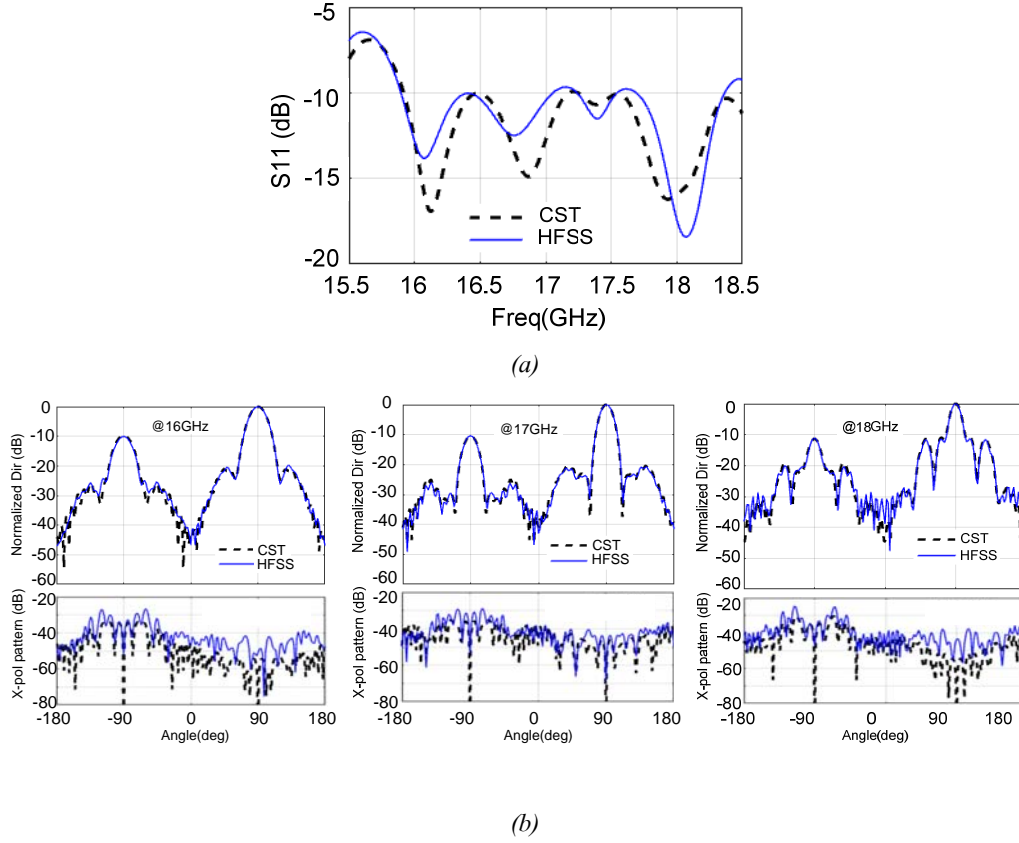


Fig. 4. Simulation results (HFSS & CST) for the ordinary GGW H-plane horn presented in Fig. 1(a). (a) Reflection coefficient (S_{11}) and (b) Radiation patterns at H-plane (co- & cross) at three frequencies over the whole bandwidth.

III. SIMULATION RESULTS

The designed antennas with the dimensions listed in TABLE I was simulated by HFSS software. The simulation results including reflection coefficient S_{11} and H-plane radiation pattern are presented in Figs. 4 & 5. Fig. 4 represents the results for the ordinary GGW H-plane horn shown in Fig. 1(a) however Fig. 5 stands for the back lobe suppressed H-plane horn presented in Fig. 1(b). In Figs. 4 & 5 the simulation results obtained by HFSS are compared with those obtained by CST and good agreement between them evaluates the simulated results.

In Fig. 4 (a) we see that the reflection coefficient is less than -10dB ($S_{11} < -10\text{dB}$) over $15.9\text{--}18.4\text{ GHz}$ which represents that the designed ordinary GGW H-plane horn antenna has the impedance bandwidth (BW) of 15.7% , which is significantly more than 1% BW of RGW horn antenna presented in [7] (Fig. 2). In Fig. 4. (b) the co- & cross polar H-plane radiation patterns at three frequencies over the antenna bandwidth are also shown and proper performance through the whole bandwidth can be observed. We see that the cross polar level at the maximum radiation angle is less than -40dB over the

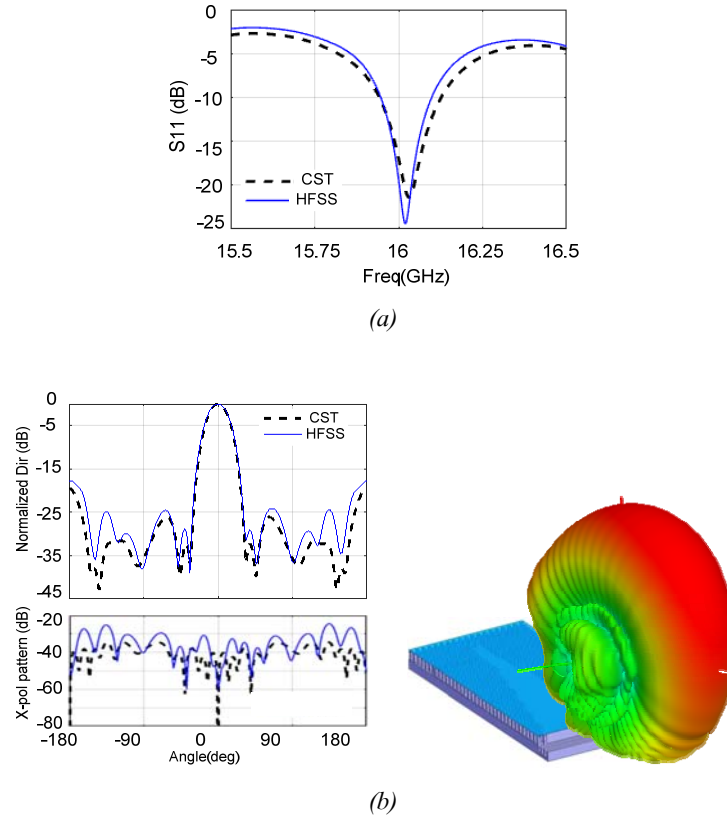


Fig. 5. Simulation results (CST & HFSS) for the back lobe suppressed GGW H-plane horn presented in Fig. 1(b).
 (a) Reflection coefficient (S11) (b) H-plane radiation pattern (co-& cross) and 3-D pattern at 16 GHz.

whole bandwidth. We can also see that the Front to back ratio (FTBR) over the band width is about 10 dB.

In Fig. 5(a) only 1% impedance bandwidth can be observed which reveals that using the corrugated surface at the antenna aperture has resulted in much reduction in antenna bandwidth. The reason is that the impedance matching between the antenna aperture and outer space is very difficult with the presence of high impedance surface at the antenna aperture. In Fig. 5(b) the co-& cross polar radiation patterns in H-plane @16GHz are shown. We see that the cross polar level at the maximum radiation angle is less than -40dB. The 3D radiation pattern at 16GHz is also illustrated in order to give the reader better imaginary about the antenna radiation performance. We see that in this case the FTBR is 18dB which shows that the backward radiation is significantly reduced compared to the case shown in Fig. 4. This fact can be also clearly seen in Fig. 6 where the H-plane radiation patterns of the mentioned antennas are compared @ 16GHz.

In the designed example three rows of corrugations were used however enhanced performance can be obtained using more corrugations at the expense of antenna size enlargement. In Fig. 7 the antenna FTBR vs number of corrugations is investigated. We see that after two rows of corrugations the backward radiation is significantly reduced.

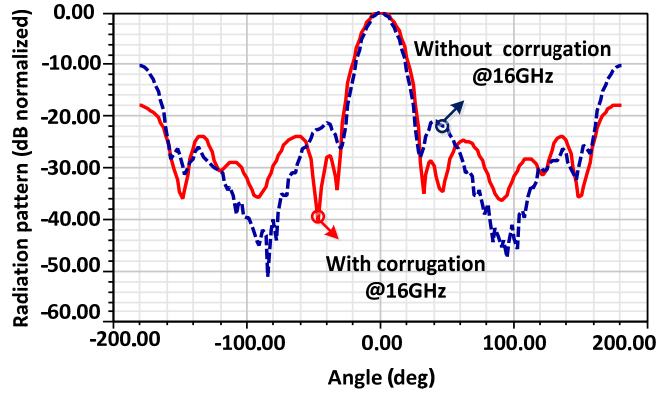


Fig. 6. Comparison between H-plane radiation patterns of antennas presented in Figs. 1(a) and (b).

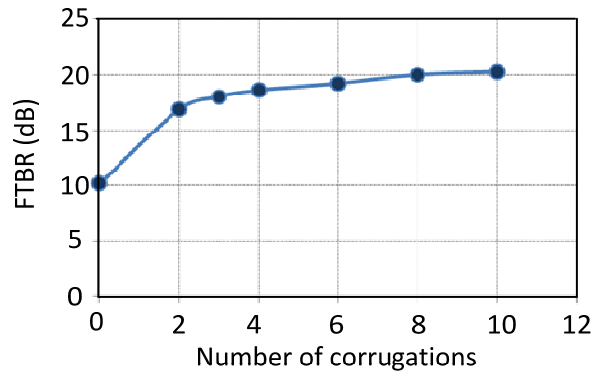


Fig. 7. Front to back ratio (FTBR) vs number of corrugations for the antenna presented in Fig. 1(b).

With three rows of corrugations the FTBR is enhanced by 8dB compared to the case no corrugation is used (i.e. Fig. 1(a)). Using more than three corrugations the backward radiation can be slightly reduced but at the expense of antenna size enhancement. We see that increasing the number of corrugations more than three does not significantly affect the backward radiation meaning that three corrugations is sufficient to completely stop the wave propagation in $\square y \square$ direction.

In TABLE II some important radiation characteristics of designed antennas are summarized and compared with those of antenna presented in [10] whose 3D view is also shown in Fig. 3. In this Table the terms $\square HPBW \square$, $\square FTBR \square$, $\square SLL \square$ and $\square BW \square$ refers to \square half power beam width \square , \square front to back ratio \square , \square side lobe level \square and \square Bandwidth \square respectively. It can be observed that in our designs, the side lobe level and backward radiation are decreased significantly which has led to gain enhancement compared to the antenna presented in [10].

Table II. IMPORTANT RADIATION PROPERTIES OF THE PROPOSED ANTENNAS COMPARED WITH THOSE OF THE ANTENNA PRESENTED IN [10]

Parameter	GGW With corrugation	GGW without corrugation	RGW horn in [10]
Gain (dB)	13.5	11.5	10.3
FTBR (dB)	18	10.1	7.15
SLL (dB)	-28.71	-21.27	-12.3

IV. CONCLUSIONS

A new *H*-plane horn antenna based on groove gap waveguide technology is presented and a method for its backlobe suppression and gain enhancement is introduced by making use of a high impedance surface at the antenna aperture. The radiation performance of presented antennas were investigated and it is observed that with the ordinary form, i.e. without backlobe suppressor, wider impedance bandwidth can be obtained compared to the RGW horn presented in [10]. However we saw that the presented backlobe suppression mechanism can significantly improve FTBR and antenna gain but at the expense of losing the bandwidth.

REFERENCES

- [1] P. S. Kildal, E. Alfonso, A. Valero Noguero, and E. Rajo-Iglesias, "Local metamaterial-based waveguides in gaps between parallel metal plates," *IEEE Antennas and Wireless Propag. Lett.*, vol. 8, pp. 84-87, 2009.
- [2] E. Rajo-Iglesias and P. S. Kildal, "Groove Gap Waveguide: A rectangular waveguide between contactless metal plates enabled by parallel-plate cut off," *EuCAP 2010 Fourth Eur. Conf. Antennas Propag.*, pp. 12-16, 2010.
- [3] A. Zaman, P. S. Kildal, and A. Kishk, "Narrowband microwave filter using high-Q groove gap waveguide resonators with manufacturing flexibility and no sidewalls," *IEEE Transactions on Components, Packaging and Manufacturing Technology*, vol. 2, no. 11, pp. 1882-1889, Nov. 2012.
- [4] P. S. Kildal, "Three metamaterial-based gap waveguides between parallel metal plates for mm/sub mm waves," *3rd Eur. Conf. Antennas Propag.*, pp. 28-32, 2009.
- [5] P. S. Kildal, A. U. Zaman, E. Rajo-Iglesias, E. Alfonso, and A. Valero-Nogueira, "Design and experimental verification of ridge gap waveguide in bed of nails for parallel-plate mode suppression," *IET Microwave. Antennas Propag.*, vol. 5, no. 3, pp. 262-270, Feb. 2011.
- [6] A. Valero-Nogueira, M. Baquero, J. I. Herranz, J. Domenech, E. Alfonso, and A. Vila, "Gap waveguides using a suspended strip on a bed of nails," *IEEE Antennas Wireless Propag. Lett.*, vol. 10, pp. 1006-10, 2011.
- [7] A. Vosoogh and P. S. Kildal, "Corporate-fed planar 60 GHz slot array made of three unconnected metal layers using a MC pin surface for the gap waveguide," *IEEE Antennas Wireless Propag. Lett.*, vol. 15, pp. 1935-1938, 2016.
- [8] A. Vosoogh, P. S. Kildal, and V. Vassilev, "Wideband and high-gain corporate-fed gap waveguide slot array antenna with ETSI class II radiation pattern in V-band," *IEEE Trans. Antennas Propag.*, vol. 65, no. 4, pp. 1823-1831, April 2017.
- [9] D. Zarifi, A. Farahbakhsh, A. U. Zaman, and P. S. Kildal, "Design and fabrication of a high-gain 60-GHz corrugated slot antenna array with ridge gap waveguide distribution layer," *IEEE Trans. Antennas Propag.*, vol. 64, no. 7, pp. 2905-2913, July 2016.

- [10] F. Ahmadfard and S. A. Razavi, "H-Plane horn antenna in ridge gap waveguide technology," *2nd Iranian Conference on Communication Engineering (ICEE)*, Shiraz, 2016.
- [11] E. Rajo-Iglesias and P. S. Kildal, "Numerical studies of bandwidth of parallel-plate cut-off realized by a bed of nails, corrugations and mushroom-type electromagnetic bandgap for use in gap waveguides," *IET Microwaves, Antennas Propag.*, vol. 5, no. 3, pp. 282-289, Feb. 2011.
- [12] A. W. Love, "Electromagnetic horn antennas," *IEEE Press selected reprint series*, New York, 1976.
- [13] M. Esquiús-Morote, B. Fuchs, J. F. Zürcher, and J. R. Mosig, "A printed transition for matching improvement of SIW horn antennas," *IEEE Trans. Antennas Propag.*, vol. 61, no. 4, pp. 1923-1930, April 2013.
- [14] M. Esquiús-Morote, B. Fuchs, J. F. Zürcher, and J. R. Mosig, "Novel thin and compact H-plane SIW horn antenna," *IEEE Trans. Antennas Propag.*, vol. 61, no. 6, pp. 2911-2920, June 2013.
- [15] P. S. Kildal, "Artificially soft and hard surfaces in electromagnetics," *IEEE Trans. Antennas Propag.*, vol. 38, no. 10, p. 1537-1544, Oct. 1990.